JOURNAL OF MATERIALS SCIENCE 33 (1998) 3615–3622

The fibre distribution of Al_2O_3/Al–Cu alloy composites

HUA-NAN LIU, KEISAKU OGI, HIROFUMI MIYAHARA
Department of Materials Science and Engineering, Kyushu University, Hakozaki 6-10-1, Higashi-ku, Fukuoka 812-81, Japan
E-mail: liu@zaiko.kyushu-u.ac.jp

Two methods which rely on direct microstructural measurements to assess the fibre distribution in alumina continuous fibre-reinforced Al–Cu alloy composites produced via an infiltration process, are outlined. The first is based on distance analysis, i.e. the distance distribution of nearest neighbours; and the second is based on fibre–cell structures. Specimens with two fibre volume fractions, 0.39 and 0.50, were employed in this study. It was found that the fibres in both kinds of specimen appear to have a rough thread-like distributions, and the local volume fraction of the fibres varies over a larger range in the specimen with lower fibre volume fraction than does that in the specimen with the larger one. Quantitative relationships between fibre distribution and the composite defects are deduced. Some data on the microsegregation of copper and the macrosegregation of eutectic phase are given in relation to the fibre distributions. The reasons for the uneven fibre distributions are also discussed.

1. Introduction

Many processes have been developed to produce the ceramic fibre-reinforced aluminium alloy matrix composites [1–3], and research on the solidification of matrix alloys in the presence of reinforcements has also been widely carried out [4–8], but only few observations of the fibre distribution in composites exist in the open literature. The control of the fibre distribution is one of the key techniques for the design and realization of proper structures and properties of composites. A knowledge of the degree of fibre clustering and classification of the influence of the uneven distribution of fibres on the structure and properties of composites, are very important in both research and applications.

Several methods had been presented for the quantitative metallographic assessments, and some of them were proposed for quantitative characterization of the distribution of reinforcements in a composite. Stone and Tsakiropoulos [9, 10] used two methods, based on the measurement of the distribution of interparticle spacings of the reinforcement, and on the Dirichlet tessellation construction, to assess the quality of the spatial distribution of reinforcements in the Al–4Cu/$20SiC_p$ composites produced via a powder metallurgy route, and found that the width of the interparticle spacing and Dirichlet cell-size distributions were a function of the level of microstructural homogeneity. They also applied a local energy dispersive X-ray analysis to the same composite, and found that the technique was sensitive to small differences in the spatial distribution of the reinforcement. Li *et al.* [11] observed the fibre distribution within metal matrix composites using matrix intercept-length measurements, and found that the fibre distribution in the composites was clustered, compared to a computer–generated random circular distribution, and the fibre distribution was influenced by the cooling rate during the solidification of the composites. W. Spitzig *et al.* [12] reported Dirichlet cell tessellation procedures by which they observed that the fibre distribution in a kind of graphite fibre-reinforced aluminium alloy was close to random. However, the characterization of spatial distribution of the reinforcement in metal matrix composite is still inadequate, and there have been few studies on the quantitative relationships between reinforcement distribution and the composite properties and microstructure.

The present work was undertaken as part of a study to characterize the microstructure and properties of alumina continuous fibre-reinforced Al–Cu alloy composite produced via unidirectional infiltration process. Composite microstructure and segregation were greatly influenced by the fibre distribution [4–8, 11]; this in turn, would greatly influence the properties of the composites because it has been well established that the tensile and compressive strength of continuously reinforced metal matrix composites were strongly dependent on the properties of the matrix and interface. The compressive strength, in particular, was very sensitive to fibre misalignment [13, 14]. The main purposes of this work were to characterize the fibre distribution in composites and to attempt to describe the quantitative relationships between fibre distribution and composite microstructure. The methods employed were distance analysis and the fibre–cell

process. These were achieved by analysing the distance distribution of nearest neighbours to determine the degree of fibre clustering, which was then used to estimate the amount of defects which often occurred in the contact area of two neighbouring fibres for non-wetting systems (the contact angle of a molten matrix alloy on the fibre is larger than 90°), and by using fibre–cell structures to determine the local volume fraction of fibres, which was then used to investigate the influence of an uneven fibre distribution on the macrosegregation of eutectic phases and the microsegregation of components. A comparison was made to determine the influence of fibre mean volume fraction on the characters of fibre clusters. The probability of application of the two methods used is also discussed. Because the fibre mean volume fractions in the continuously reinforced metal matrix composite produced via the infiltration process are generally in the range 0.35–0.55, with volume fractions of 0.39 and 0.50, respectively, were chosen for the present studies.

2. Experimental procedure

2.1. Samples

Al_2O_3 continuous fibre (γ-Al_2O_3, diameter 17 μm) reinforced Al–4.43 wt % Cu, Al–6.48 wt % Cu and Al–4.45 wt % Cu–1.54 wt % Mg alloys are used in the present studies. Specimens with the dimensions 10 mm diameter × 40 mm were fabricated by a unidirectional infiltration process in a vacuum condition of 2–3 Pa and then solidified at the cooling rate of $0.43\,^{\circ}C\,s^{-1}$ with a growth rate of about $0.31\,mm\,s^{-1}$. Micro-observation and microanalysis were performed on a typical cross-sectional area at the central part of as-cast specimens with the aid of an optical microscope and a Hitachi X-650 scanning electron microanalyser. Details of the infiltration process were given elsewhere [15].

2.2. Methods of measurement

The measurements were carried out on typical optical micrographs of cross-sections at the central part of composite specimens with the aid of a Macintosh image analysis system.

The analysis procedure of nearest neighbour distance were recording the coordinate centroid of each fibre, calculating the nearest, second nearest and third nearest surface to surface distance by computer; the fibre distance distributions were then plotted.

The processes of generating fibre–cell structures were keeping the fibre centroids fixed, allowing the fibres to grow bigger and bigger at a constant speed until the interfibre spaces are all occupied, then the fibre surfaces made contact with their neighbours forming cell-like boundaries. The details are as follows:

Macintosh HD
→ Desk scan
→ Preview
→ Zoom
→ Final (save)
→ NIH image
→ NIH image 1.59/fat
→ File → open
→ Options → Density slice
→ Process → Binary → Make binary
→ Process → Plugln filters → Invert
→ Process → Binary → Skeletonize
→ Analyse → Measure → ···

Fig. 1 shows optical micrographs of the composite (Fig. 1a) and its fibre–cell structures (Fig. 1b). It can be seen that the fibre–cell structure is different from the Dirichilet cell tessellation, the latter, being made up of perpendicular bisectors of lines joining particle centroids, always gives linear cell boundaries [16, 17] and fibre–cell structures generated by the fibre growth method would have some irregular cell boundaries.

The fibre–cell process, as well as the Dirichilet cell process, would be the final method in determining fibre micro-distributions, as each cell only contains one corresponding fibre. Measuring the area of individual cells by computer, the fibre local volume fractions (or area fraction) in their corresponding cells are calculated from

$$V_{fc} = S_f/S_c \tag{1}$$

where V_{fc} is fibre's volume fraction in a fibre–cell, S_f and S_c are the cross-sectional areas of the fibres and of their corresponding cells, respectively.

It is obvious that edge errors will be present due to the limitation of the photo width. For the distance analysis method, fibres at the edge of the photos are considered to have their nearest neighbouring fibres only within the photo, although they could be on the outside. Increasing the size of the photographed area would decrease this kind of edge error. In the present discussion, the chosen photos cover a composite specimen area of $240 \times 340\,\mu m^2$, and edge errors are not considered. For the fibre–cell process, the edge error can be simply avoided by discounting the edge cells.

3. Results

3.1. Neighbouring distance distribution of fibres

The probabilities (the number of fibre nearest-neighbour distances or near-neighbour distances in a specified range) versus distance range for the specimen of fibre volume fraction of 0.39, are shown in Fig. 2, indicating that most of the fibres are clustered in this specimen. About 58% fibres have their nearest neighbours within a distance range of 0.5μm (Fig. 2a), while the others are in the range from 0.5–10.5 μm. The distribution of second nearest distance (Fig. 2b) ranges from 0–19μm with a larger fluctuation, the majority of them being concentrated within the 0–4 μm range, and the probability of the 0–0.5 μm range decreased to 13%. In the case of third nearest distance distribution (Fig. 2c), the majority are within the 2.5–12 μm range, only 0.9% fibres have their third nearest neighbour within the 0.5 μm distance range. A comparison of probabilities for the nearest- and the near-distance arrangements indicates that most of the fibres are

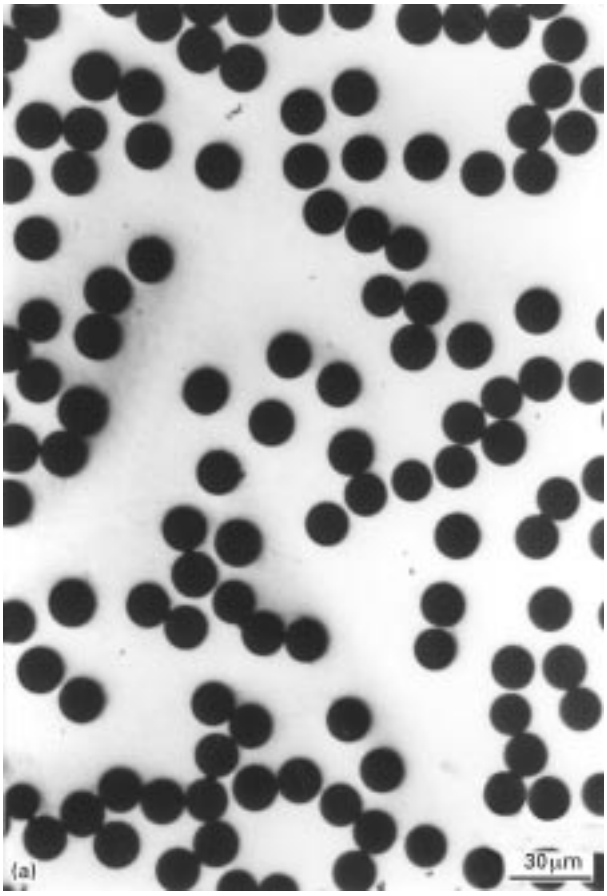

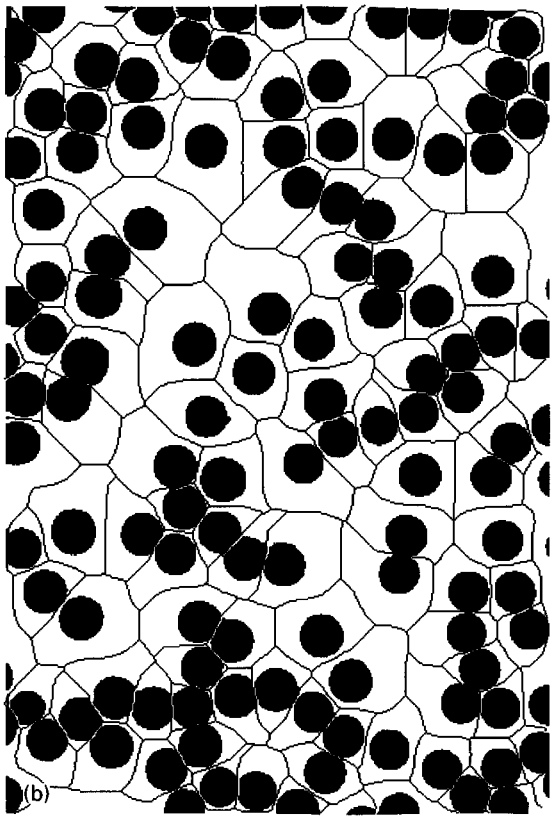

Figure 1

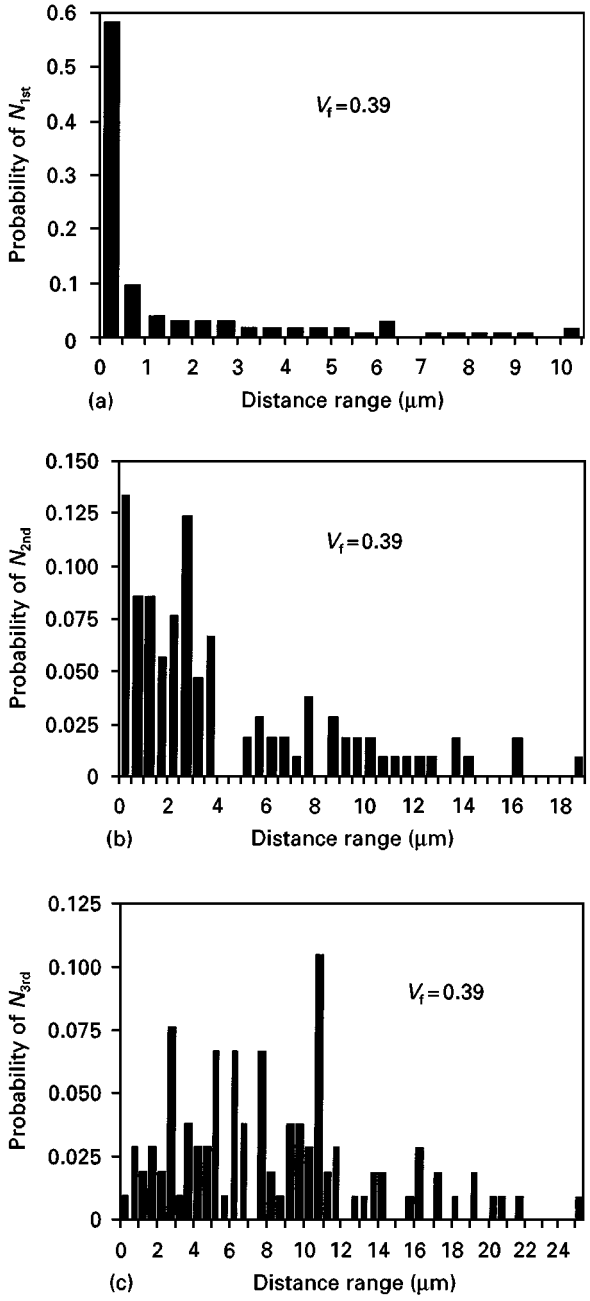

Figure 2

clustered in this specimen and the majority of them have two neighbours within the 0.5 μm distance range, but they seldom have third neighbours within this distance range; i.e. most of the fibres are clustered and the clusters are roughly in thread-shaped structures, this can also be seen in the photos (Fig. 1a).

Distance ranges for the 0.50 V_f specimen shown in Fig. 3 are similar to those for the 0.39 V_f specimen. In this case, the distance distribution for the nearest, second- and third- nearest neighbours are concentrated in the ranges 0–3.5, 0–4, and 0–7.5 μm, respectively. The probabilities of the 0.5 μm distance range for the nearest, second- and third- nearest neighbours are 70.8%, 20.1% and 3.5%, respectively, indicating that clusters in this specimen also exhibit thread-like structures, and also showing that the increase of fibre volume fraction has aggravated the degree of clustering.

3.2. Distribution of fibre local volume fraction

The probabilities (the number of fibre local volume fractions in a specified range) versus fibre local volume

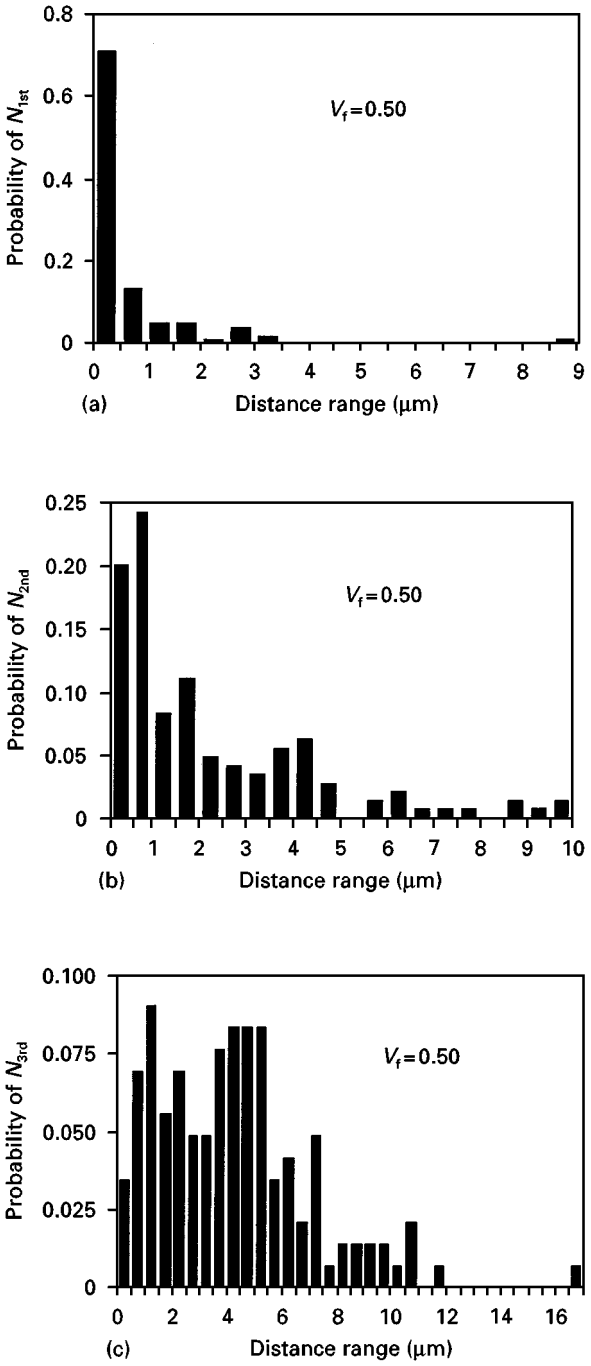

Figure 3

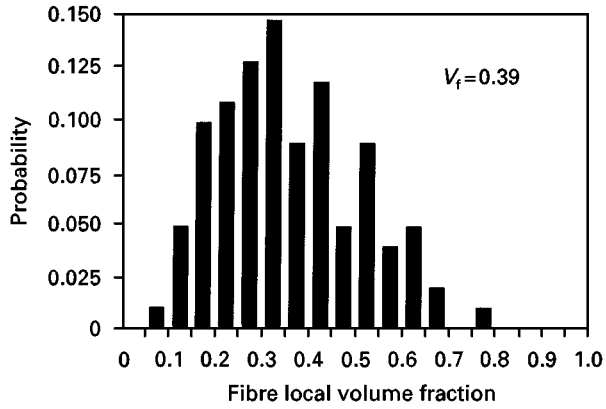

Figure 4

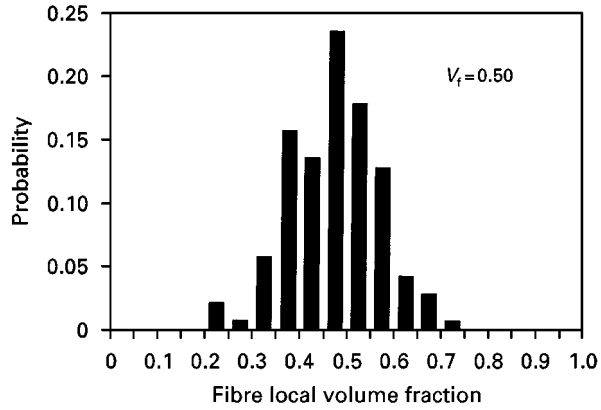

Figure 5

(or area) fraction range, are shown in Figs 4 and 5. In the specimen with a general volume fraction of 0.39 (Fig. 4), the local volume fraction varies from 0.15– 0.85, and the maximum probability is about 14.7%, covering a range of 0.35–0.40 volume fractions. However, in the 0.50 V_f specimen, the fibre local volume fractions were concentrated in the range of 0.25–0.80 with a maximum probability of about 23.6% in the range 0.50–0.55 (Fig. 5). These indicate that the smaller the fibre general volume fraction, the greater is the uneven fibre distributions which would arise, because the decrease of volume fraction allows more room for the fibres to move or to be rearranged during the infiltration and solidification processes.

4. Discussion

4.1. Characteristics of fibre clusters

Many factors could contribute to an uneven fibre distribution, such as the preparation of preforms, and the infiltration and solidification processes. The formation of thread-like fibre clusters can also be interpreted by these factors. Firstly, there was originally an uneven distribution in the fibre preform, i.e. the interfibre space size was irregular. During the infiltration process, the large interfibre spacings were infiltrated first and so the fibres surrounding these interspaces were then pushed aside by the perpendicular pressure of the infiltrated liquid metal (as sketched in Fig. 6), which enhanced the uneveness of distribution and made more fibres surround the infiltrated spaces (similar evidence was given by Mortensen [18]). Thus, the fibres either surrounding or on the surface of the infiltrated liquid metals began to take on thread-like characters. With increasing liquid pressure, the narrower interfibre spaces were also gradually infiltrated until infiltration of the preform was complete. The uneveness of the distribution was further enhanced during the solidification process: the solidification of the liquid metal began in the larger interfibre spaces (which are surrounded by the thread-like clusters of fibres); it then proceeded to the fibre surface and pushes them to the last solidified regions, which made the fibre clusters more inclined to form thread-like structures.

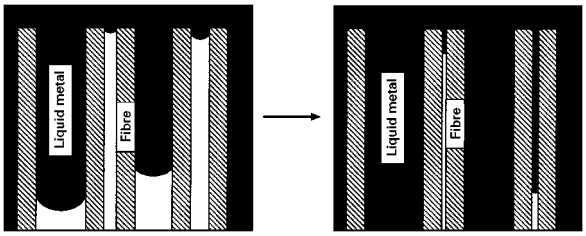

Figure 6

4.2. Application of the fibre distance distribution

For non-wetting systems, defects will occur between neighbouring fibres if they contact each other or the distance between them is shorter than the critical distance [15, 19]. The thread-like structure of fibre clusters allows estimation of the amount of defects in composites by analysis of the fibre distance distributions, because the defects can be considered to be points between contacted or nearly contacted neighbouring fibres. Postulating that the fibre distribution in the cross-section of the composites is in the form of thread-shaped clusters or in dendritic structures, and that neither threads nor the trunk and branches of dendrites are closed circuits, for a given critical distance, the number of defects in a unit cross-sectional area of a composite can be simply estimated as follows.

First, the following definitions are made:

N is the number of total fibres in a unit area;

N_{1st} is the number of the fibres which have at least one neighbour within a critical distance;

N_{2nd} is the number of the fibres which have at least two neighbours within a critical distance.

N_{3rd}, N_{4th}, N_{5th} and N_{6th} are also defined by this rule (in a narrow distance range, the number of neighbouring fibres surrounding the same fibre is not more than 6).

$N_{i=1,2,\ldots,n}$ is the number of clusters consisting of i fibres, each of which has at least one neighbour within the critical distance, i.e. the N_1 represents the number of dissociated fibres, and the N_2 is the number of the clusters consisting of two fibres etc.

Other relations are

$$N = N_1 + 2N_2 + 3N_3 + \cdots + nN_n \quad (2)$$

$$N_{1st} = 2N_2 + 3N_3 + \cdots + nN_n \quad (3)$$

In the case when $N_{3rd} = N_{4th} = N_{5th} = N_{6th} = 0$,

$$N_{2nd} = N_3 + 2N_4 + \cdots + (n-2)N_n \quad (4)$$

Considering the influence of N_{3rd}, Equation 4 becomes

$$N_{2nd} + N_{3rd} = N_3 + 2N_4 + \cdots + (n-2)N_n \quad (5)$$

and so on; if the N_{3rd}, N_{4th}, N_{5th}, and N_{6th} are all considered, then

$$N_{2nd} + N_{3rd} + N_{4th} + N_{5th} + N_{6th} = N_3 + 2N_4 + \cdots + (n-2)N_n \quad (6)$$

In addition, the number of defects, N_d, in the unit area is

$$N_d = N_2 + 2N_3 + \cdots + (n-1)N \quad (7)$$

Combining Equations 3, 6 and 7 yields

$$N_d = (N_{1st} + N_{2nd} + N_{3rd} + N_{4th} + N_{5th} + N_{6th})/2 \quad (8)$$

and so the probability of the defect number ($P[N_d]$) can be estimated as

$$P[N_d] = (P[N_{1st}] + P[N_{2nd}] + \cdots + P[N_{6th}])N/2 = 2(P[N_{1st}] + P[N_{2nd}] + \cdots + P[N_{6th}])V_f/(\pi d_f^2) \quad (9)$$

where $P[N_{1st}]$, $P[N_{2nd}]$, …, $P[N_{6th}]$ are the probabilities of N_{1st}, N_{2nd}, …, N_{6th}, respectively, and d_f is the diameter of fibres.

In real situations, $P[N_{4th}]$, $P[N_{5th}]$ and $P[N_{6th}]$ are very small, and are usually discounted in calculation of the defect number. On the other hand, if $P[N_{4th}]$, $P[N_{5th}]$ and $P[N_{6th}]$ cannot be ignored, then the dendritic branches in fibre clusters easily contact each other, making the calculation of defects more complex and difficult.

In Al_2O_3 fibre-reinforced Al–Cu single phase alloy composites, both Al_2O_3 fibres and θ-phase precipitated from non-equilibrium solidification are pushed into the last solidified arm spaces with the θ-phases chaining fibres to form thread-like or dendritic clusters. Even the areas between very close neighbouring fibres are entirely infiltrated, and the presence of θ-phase would weaken this area. Therefore, to investigate the numbers of dissociated fibres and of those in the θ-phases, binding of clusters is also important. For a given distance range, the probability of dissociated fibres number ($P[N_1]$) and that of clustered fibres ($P[N_c]$) in a unit cross-sectional area can be estimated as

$$P[N_1] = 4(1 - P[N_{1st}])V_f/(\pi d_f^2) \quad (10)$$

$$P[N_c] = 4(P[N_{1st}])V_f/(\pi d_f^2) \quad (11)$$

Fig. 7 shows a scanning electron micrograph of a defect between two contacted fibres; this kind of defect will no doubt harm the mechanical properties of the composite. Even if the contacted (or nearly contacted) regions between two neighbouring fibres were completely infiltrated, they would still be the weakest regions of the composite due to the effect of stress concentration and the presence of θ-phases (for the Al_2O_3/Al–Cu single-phase alloy composites). Evidence from present studies given in Fig. 8 shows that a crack was generated from the contacted area of two neighbouring fibres on the fracture surface of an Al_2O_3/Al–4.43 wt % Cu composites after tensile testing. The number of this kind of "weak points" can also be estimated from Equation 9 by choosing a certain distance range.

4.3. Application of fibre–cell structures

Except for the description of fibre local volume fractions, the fibre–cell structures are also related

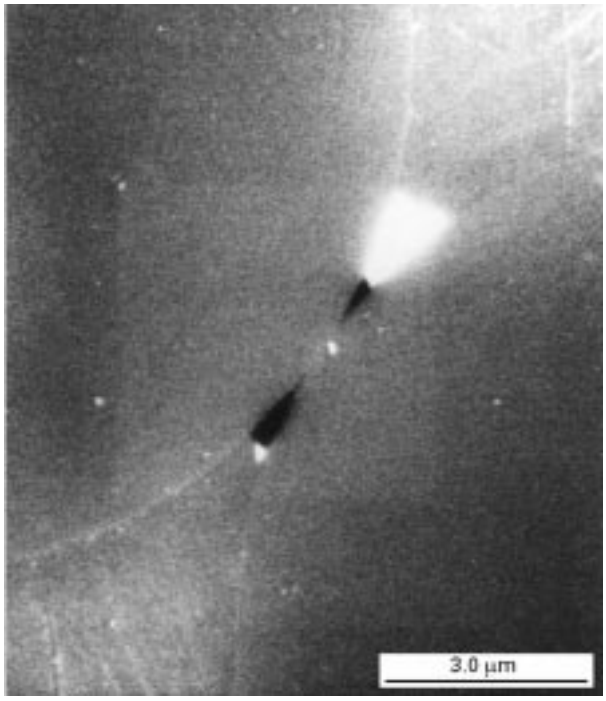

Figure 7

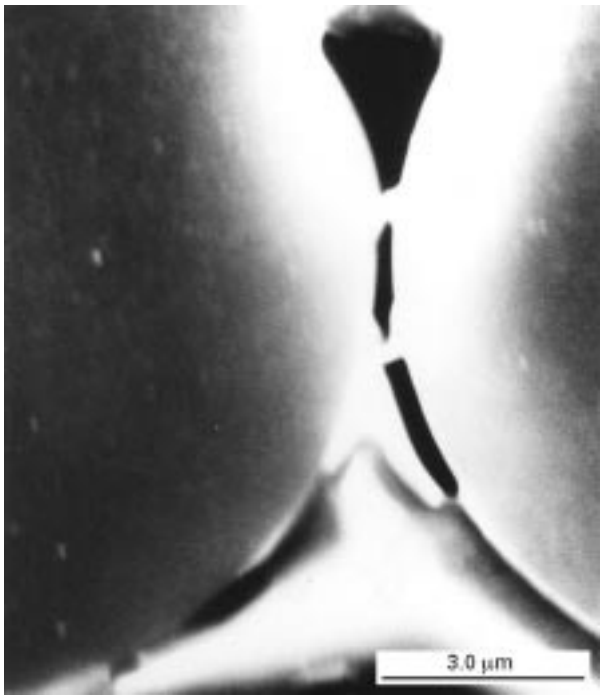

Figure 8

quantitatively to the microstructure and microsegregation of composites. Previous studies [5–8, 20] confirmed that the nucleation of the matrix alloy takes place away from the fibre surface and starts within a large interstice first, and then proceeds in the smaller interstices. They also revealed that α-phase crystals grow away from fibres, resulting in a minimum concentration of solute in the centre of the interfibre spaces and a maximum concentration near fibres as shown by the electron probe microanalysis (EPMA) line profile of copper across a large interfibre space (Fig. 9). The uneven distribution of fibres makes this

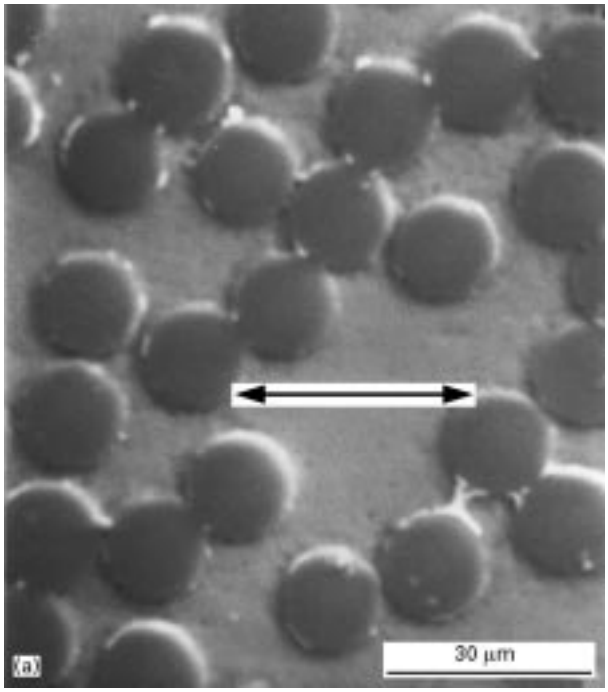

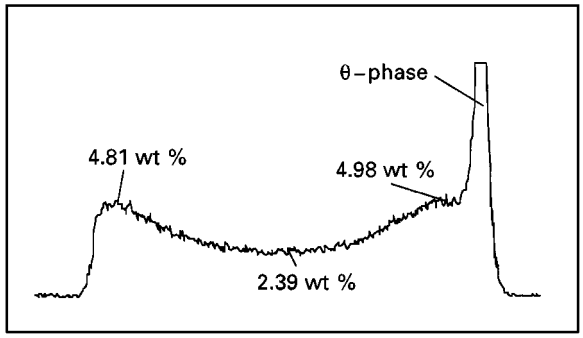

Figure 9

segregation more serious, as shown in Fig. 10, where the minimum concentration of copper in larger interfibre spaces is lower than that in smaller ones, where the width of the interfibre space is related to the intercept-length of the matrix in their corresponding cells. It can be postulated that growth of α-phase ejects solutes to the later-solidified regions and causes the smaller interfibre space to solidify at a higher content of solutes. A computer simulation of heat flow and solute distribution of Al_2O_3/Al–Cu alloy composites, performed by our research group [21], suggested the possibility of a delay of solidification and an increase of copper content in regions where fibres are densely distributed.

The fibre macro-segregation would affect the distribution of eutectic phases (or θ-phases). It was impossible to measure the area fraction of eutectic phase in the individual cells, due to the limitation of our image analysis system. However, an attempt was made to characterize the relationships between the distribution of fibres and that of eutectic phases using the general volume (or area) fraction measured in an area of $120 \times 180\,\mu m^2$ instead of that in the cells. The results are shown in Fig. 11, indicating that the eutectic phases are concentrated in the regions where fibres are densely distributed.

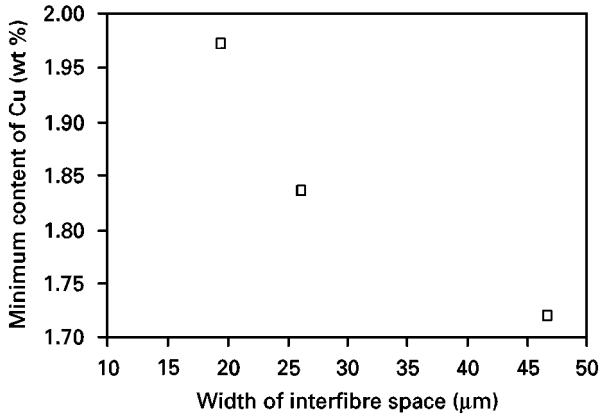

Figure 10

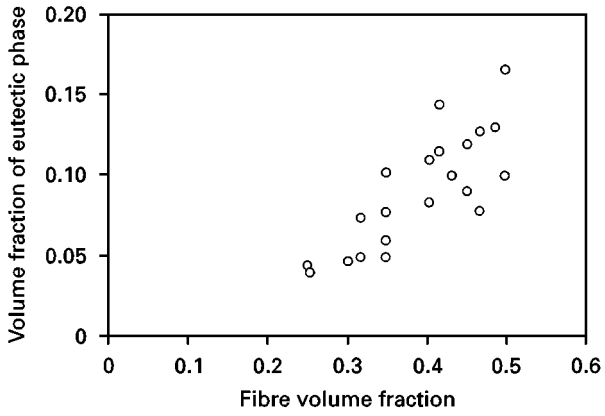

Figure 11

The fibre–cell structure could also be used in the prediction of the mechanical properties of a composite. It is well known that the tensile and compressive strength of continuously reinforced composites are a function of the fibre volume fraction, i.e.

$$\sigma = f(V_f) \tag{12}$$

If the fibres are very unevenly distributed, the strength calculated by using the mean volume fraction of fibres would increase in error. In a fibre–cell structure, the matrix in this cell can be considered only the influence its corresponding fibre, and so the introduction of a fibre local volume fraction would improve the accuracy of calculation.

Comparing the fibre distance distribution and fibre–cell structures, the former gives an accurate distance relationship of neighbouring fibres, but has no relevance to interfibre spaces, while the latter has good relevance to matrix intercept length, but is not sensitive to the distance between fibres.

5. Conclusions

1. The fibre distribution in Al_2O_3/Al–Cu alloy composites of two kinds of volume fraction were estimated by using the distance analysis method, and it was found that fibres were more concentrated in specimens with a higher volume fraction, and fibres in both kinds of specimen appears to have a rough thread-like distribution which was considered to be the result of the fabrication processes.

2. An uneven fibre distribution affects the composite defects formed in the area of two contacting fibres (or those having a neighbouring distance smaller than the critical distance needed to form a defect). For the fibres distributed in thread-like or dendritic structures which were not closed circuits, the number of defects in a unit area can be estimated by measuring the distribution probabilities of the nearest, and second- and third-nearest distances, i.e.

$$P[N_d] = (P[N_{1st}] + P[N_{2nd}] + \cdots + P[N_{6th}])N/2$$
$$= 2(P[N_{1st}] + P[N_{2nd}] + \cdots + P[N_{6th}])V_f/(\pi d_f^2)$$

and the number of dissociated fibres ($P[N_1]$) and that of clustered fibres ($P[N_c]$) in this area can be estimated as

$$P[N_1] = 4(1 - P[N_{1st}])V_f/(\pi d_f^2)$$
$$P[N_c] = 4(P[N_{1st}])V_f/(\pi d_f^2)$$

3. Proof has been given that cracks can be generated from the contact area between two neighbouring fibres under a stress concentration during the tensile testing of composites.

4. Fibre distribution was also investigated by using the fibre–cell process, with the result that the fibre local volume fraction was found to vary over a larger range in the specimen with a lower V_f than that with a higher volume fraction.

5. The uneven distribution of fibres influenced the microsegregation and microstructure of composites. In the same specimens, the minimum concentration of copper across the larger interfibre spaces was smaller than that in the smaller interspaces; the eutectic phase (or θ-phase) was roughly concentrated in the regions where fibres were densely distributed.

Acknowledgements

We thank Mr Wakasugi for his assistance in operating the scanning electron microanalyser, Mrs Murai for her work on the chemical analysis of the matrix alloys, and Mr Moriguti and Mr Haraoka whose experimental work led to Fig. 10 of this paper.

References

1. T. W. CLYNE and J. F. MASON, *Metall. Trans.* **18A** (1987) 1519.
2. T. W. CHOU, A. KELLY and A. OKURA, *Composites* **16** No.(3) (1985) 187.
3. J -Q. JIANG, A -B. MA, H -N. LIU and R -S. TAN, *Mater. Sci. Technol.* **10** (1994) 783.
4. H -N. LIU, H. MIYAHARA and K. OGI, edited by G. Sun et al. "The Fifth Asian Foundry Congress" (Southeast University Press, Sept. 1997, P. R. China) pp. 425–32.
5. Q. F. LI, D. G. McCARTNEY and A. M. WALKER, *J. Mater Sci.* **26** (1991) 3565.
6. A. MORTENSON, M. N. GUNGOR, J. A. CORNIE and M. C. FLEMING, *J. Metals* **38** (1986) 30.
7. A. MORTENSON, J. A. CORNIE and M. C. FLEMINGS, *Metall. Trans.* **19A** (1988) 709.
8. N. F. DEAN, A. MORTENSON and M. C. FLEMING, *ibid.* **26A** (1995) 2141.

9. C. STONE and P. TSAKIROPOULOS, *Mater. Sci. Technol.* **11** (1995) 213.
10. *Idem., ibid.* **11** (1995) 222.
11. Q. F. LI, D. G. McCARTNEY, N. L. LON, *J. Mater. Proc. Technol.* **51** (1995) 244.
12. W. A. SPITZIG, J. F. KELLY and O. RICHMOND, *Metallography* **18** (1985) 235.
13. H. E. DEVE, *Acta Mater.* **45** (1997) 5041.
14. K. YAMADA, S. SEKIGUCHI, T. HANAMURA and T. INOUE, *J. Jpn Inst. Metals* **59** (1995) 1108.
15. H -N. LIU, H. MIYAHARA and K. OGI, *Mater. Sci. Technol.*, **14** (1998) 292.
16. P. J. WRAY, O. RICHMOND and H. L. MORRISON, *Metallography* **16** (1983) 39.
17. J. R. BROCKENBROUGH, W. H. HUNT Jr, O. RICHMOND, *Scripta Metall. Mater.* **18** (1985) 235.
18. A. MORTENSON, *Mater. Sci. Eng.* **A135** (1991) 1.
19. A. MORTENSON and J. A. CORNIE, *Metall. Trans.* **18A** (1987) 1160.
20. Q. F. LI and D. G. McCARTNEY, *J. Mater. Proc. Technol.* **51** (1995) 135.
21. K. OGI, H. MIYAMURA and H -N. LIU, "Analysis on the micro heat transmission and crystal growth of Al-Cu alloy in the presence of ceramic fibers". The Grant-in-Aid for Scientific Research on Priority Areas sponsored by the Ministry of Education, Science, Sports and Culture, Japan, "Development of Micro-Heat Transfer in Manufacturing and Processing of New Materials", Final Report, March 1997, pp. 183–92.

Received 9 June 1997
and accepted 22 April 1998